NUCL SCI TECH (2018) 29:111
https://doi.org/10.1007/s41365-018-0451-8

CrossMark

Total ionizing dose and synergistic effects of magnetoresistive random-access memory

Xing-Yao Zhang[1,2] · Qi Guo[1,2] · Yu-Dong Li[1,2] · Lin Wen[1,2]

Received: 27 September 2017 / Revised: 2 January 2018 / Accepted: 15 January 2018 / Published online: 4 July 2018
© Shanghai Institute of Applied Physics, Chinese Academy of Sciences, Chinese Nuclear Society, Science Press China and Springer Nature Singapore Pte Ltd. 2018

Abstract A magnetoresistive random-access memory (MRAM) device was irradiated by ^{60}Co γ-rays and an electron beam. The synergistic effect of this on the MRAM was tested with an additional magnetic field during irradiation, from which the total ionizing dose (TID) and the synergistic damage mechanism of MRAM were analyzed. In addition, DC, AC, and functional parameters of the memory were tested under irradiation and annealing via a very large-scale integrated circuit test system. The radiation-sensitive parameters were obtained through analyzing the data. Because of the magnetic field applied on the MRAM while testing the synergistic effects, shallow trench isolation leakage and Frenkel–Poole emission due to synergistic effects were smaller than that of TID, and hence radiation damage of the synergistic effects was also lower.

Keywords Magnetoresistive random-access memory · Total ionizing dose · Synergistic effect

This work was supported by the National Natural Science Foundation of China (No. 11705276) and the West Light Foundation of the Chinese Academy of Sciences (No. CAS-LWC-2017-2).

✉ Xing-Yao Zhang
zxy@ms.xjb.ac.cn

1 Key Laboratory of Functional Materials and Devices for Special Environments, Xinjiang Technical Institute of Physics and Chemistry, Chinese Academy of Sciences, Ürümqi 830011, China

2 Xinjiang Key Laboratory of Electronic Information Material and Device, Ürümqi 830011, China

1 Introduction

Magnetoresistive random-access memory (MRAM) is a new nonvolatile memory technology that promises unlimited endurance and faster writing speeds compared to other memory technologies currently available in the market. Hence, MRAM has received considerable attention for commercial and military applications. MRAM uses a magnetic tunnel junction (MTJ) for data storage. Figure 1 shows the structure of an MRAM cell. The MTJ is formed from two ferromagnetic plates—a magnetic free layer and a magnetic pinned layer—each of which holds a magnetic field. A tunnel barrier separates the two plates by a thin oxide layer. A bit line passes above the MTJ, while write lines run below the MTJ. The magnetic pinned layer is a permanent magnet that is set to a fixed polarity; the magnetic field in the magnetic free layer is influenced by the write and bit lines. The orientation of the magnetic field can be changed by the direction of current in the bit line. If both plates have the same polarity, the resistance of MTJ is low due to the magnetic tunneling effect, and the MTJ is considered to store a "1". When the plates are at opposite polarity, the resistance is high; thus the MTJ stores a "0".

MTJ is written by magnetic fields; in other words, the MRAM is easily affected by strong magnetic fields. Strong magnetic fields from various astronomical bodies in space, solar flares, and the magnetic torque of spacecrafts would affect the reliability of MRAM devices. Table 1 lists some values of magnetic field strengths found in the universe [1]. At the same time, electrons and protons in the Van Allen belt add to the total ionizing dose (TID) on MRAM devices in space. MRAM is influenced by synergistic effects, which blend the total ionizing dose with the magnetic field in real outer space environments.

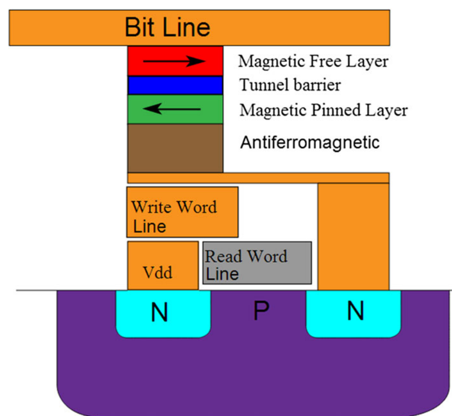

Fig. 1 (Color online) Structure of an MRAM cell

Table 1 Various magnetic field strength values

Position	Magnetic field (G)
Galaxy magnetic field	10^{-5}
Earth magnetic field	$\sim 5 \times 10^{-2}$
Solar magnetic field	$\sim 5 \times 10$
Magnetic torque in a spacecraft	$\sim 4 \times 10^{2}$
Solar flares	$\sim 5 \times 10^{3}$
Neutron star	10^{11}

Radiation damage on MRAM has been investigated since the first MRAM application was proposed. Radiation effects, as well as the mechanisms surrounding TID [2–7], single event latchup (SEL) [2–4], single event upset (SEU) [3, 5, 8–11], single event transient (SET) [9], and single event functional interrupt (SEFI) [9], have been tested and analyzed; however, the synergistic effects of radiation and magnetic fields combined have not yet been considered. The purpose of this work is to analyze synergistic effects, and whether that decreases, or enhances the radiation damage on MRAM.

2 Experimental description and result

MR25H10 (Everspin) memory is used. The MRAM is organized as 131,027 × 8 bits, with its SPI (serial peripheral interface) interface having up to 40 MHz clock rate.

The TID test was done at the Xinjiang Technical Institute of Physics and Chemistry, Chinese Academy of Sciences, using a ^{60}Co γ-radiation source, and an electron beam from an accelerator. The dose rates of the two radiation sources were very close: 0.78 Gy(Si)/s for the ^{60}Co γ source, and 0.75 Gy(Si)/s for the electron beam, which were selected according to the MIL-STD-883 J method 1019.9; 0.75 Gy(Si)/s was the closest to its suggested dose of 0.5 Gy(Si)/s. For the TID test, the MRAM was in static test mode, and all inputs were set at a fixed bias of 3.3 V. The test of synergistic effects was performed similarly, with the only difference being the addition of a magnetic field on the MRAM. The magnetic field was generated by a bulk iron nickel permanent magnet behind the MRAM. The magnetic intensity was tested by a handheld Gauss meter on the MRAM surface, which measured about 250 G of horizontally, and 150 G vertically. It was ensured that all memories were functioning properly under that magnetic intensity. Electrical parameters were tested with digital chip testing system data from the following parameters recorded between radiation levels: standby current, I_{SB}; write operation current, I_{DDW}; read operation current, I_{DDR}; highest output voltage, V_{OH}; lowest voltage, V_{OL}; input leakage current, I_{LI}; output leakage current, I_{LO}; SCK (serial clock) high time, t_{WH}; the number of errors; and functional tests. The sequence of the functional tests was, read “55”, write “00”, read “00”, write “FF”, read “FF”, write “55”, read “55”.

Tests of TID and synergistic effects exhibited reading errors at 400 Gy(Si) for various radiation sources. However, the number of errors when reading the first “55” was different (see Table 2); more read errors were observed for TID than due to synergistic effects. All memories restore functional within 24 h at room temperature annealing.

The radiation-sensitive parameters were I_{SB}, I_{DDW}, and I_{DDR}. Figures 2 and 3 show the variation of current with the accumulated dose and with annealing time for the two radiation sources. Regardless of the radiation source, the current values increased with dose, reaching a maximal value, before falling due to functional failure; however, TID exhibited larger current values than those with synergistic effects at 400 Gy(Si).

3 Discussion

Because MTJ has good radiation toleration, it could work well under irradiation [12–14]. However, the performance of CMOS peripheral control circuits deteriorated due to irradiation, and therefore, the function of memory failed immediately. Radiation introduced a large number of oxide trapped charges, leading to shallow trench isolation

Table 2 Number of read errors in test

Numbers of errors	^{60}Co γ source	Electron beam
TID	23,840	101,099
Synergistic effect	73	8864

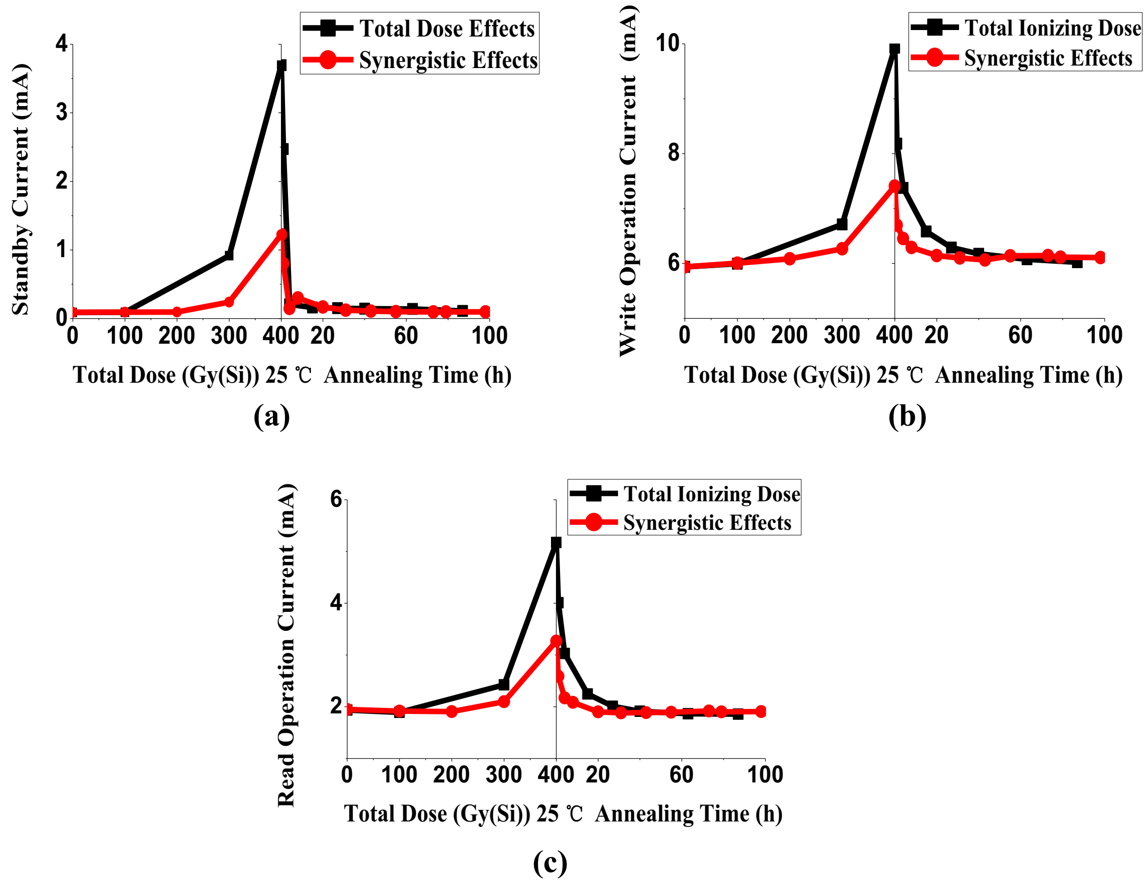

Fig. 2 (Color online) Variation of current with ^{60}Co γ-radiation dose, and annealing time for **a** I_{SB}, **b** I_{DDW}, and **c** I_{DDR}

(STI)-induced leakage [15, 16], which was the primary reason for the deterioration. Therefore, the functional failure of MRAM resulted from CMOS peripheral control circuit rather than the MTJ. The MRAM then began to restore function after the oxide trapped charges were annealed out.

Figures 2 and 3 illustrate the change in current against TID at different radiation sources. The rise in current was not only due to STI leakage, but also MTJ leakage. Schottky emission was a dominant part of MTJ leakage before radiation, where the current density, J_{SE}, was obtained for Schottky emission.

$$J_{SE} = A^{*}T^{2}\exp\left[\frac{-q(\Phi_{B} - \Delta\Phi_{SE})}{kT}\right], \tag{1}$$

$$\Delta\Phi_{SE} = \frac{1}{2}\left(\frac{q}{\pi\kappa_{r}\varepsilon_{0}}\right)^{\frac{1}{2}}E^{\frac{1}{2}} \equiv \beta_{S}E^{\frac{1}{2}}, \tag{2}$$

where A^{*} is the effective Richardson constant, T is temperature, q is the elementary charge, Φ_{B} is the barrier height of the Fermi level of the injecting metal, $\Delta\Phi_{SE}$ is due to image-force lowering [17, 18], κ_{r} is the dynamic dielectric constant, ε_{0} is the permittivity in vacuum, k is Boltzmann's constant, and E is electric field. Traps were generated more and more in the oxide layer of MTJ with the accumulating dose. With a positively applied bias to the electrode, electrons can tunnel first into the trap states, and then into the electrode, and Frenkel–Poole emission became apparent [15, 19]. The barrier height of Frenkel–Poole emission was the depth of the trap potential well, and the current density, J_{FPE}, was obtained for Frenkel–Poole emission.

$$J_{FPE} = E\exp\left[\frac{-q(\Phi_{T} - \Delta\Phi_{FPE})}{kT}\right] \tag{3}$$

$$\Delta\Phi_{FPE} = \left(\frac{q}{\pi\kappa_{r}\varepsilon_{0}}\right)^{\frac{1}{2}}E^{\frac{1}{2}} \equiv \beta_{FPE}E^{\frac{1}{2}} = 2\beta_{S}E^{\frac{1}{2}} = 2\Delta\Phi_{SE} \tag{4}$$

Denoting the barrier reduction by $\Delta\Phi_{FPE}$, the barrier reduction was larger here than in the case of Schottky emission by a factor of 2, as the barrier lowering was twice as large due to the immobility of the positive charges [17]. Frenkel–Poole emission may dominate during exposure to ionizing radiation, so MTJ leakage increased as Frenkel–Poole emission increased.

The function of MRAM failed at 400 Gy(Si) to TID, and synergistic effects, however, other parameters, such as current, and the number of errors prove that the radiation

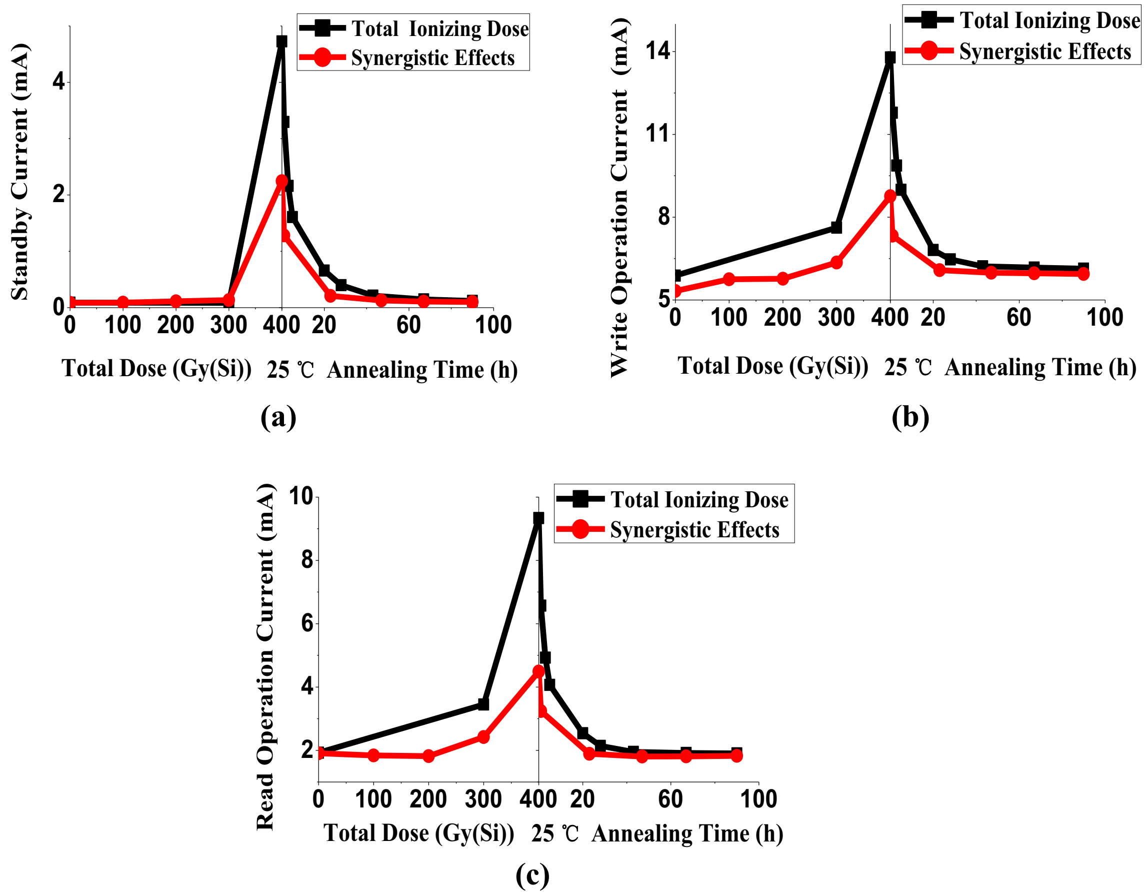

Fig. 3 (Color online) Variation of current with electron beam dose, and annealing time for **a** I_{SB}, **b** I_{DDW}, and **c** I_{DDR}

damage of synergistic effects was less than that of TID. An experiment with a vertically oriented magnetic field would explain that phenomenon. With TID, the electrons are ejected from ionizing particles and swept by the electric field fast out of the oxide layer. On the other hand, the holes are less mobile and are, therefore, trapped, leading to the creation of oxide trapped charges. With synergistic effects, both magnetic and electric fields are applied simultaneously; hence, all electrons cannot be swept out of the oxide immediately. Rather, they move along a curved path because electric field is perpendicular to the vertically oriented magnetic field at same time, as shown in Fig. 4. The net effect is that these electrons had an average "drift" in the direction of $E \times B$ [20]; Fig. 5 shows the drift motion in the oxide layer. The electrons which drift through the oxide recombine with holes, decreasing the number of holes transformed to oxide trapped charges. As a result, STI leakage, and Frenkel–Poole emission were smaller than that of TID, therefore exhibiting lower parameter degeneration.

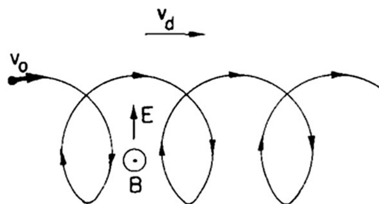

Fig. 4 Path of an electron through simultaneous electric and magnetic fields [18]

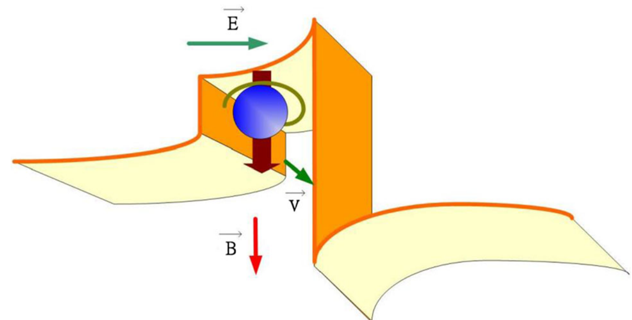

Fig. 5 (Color online) Electron drift in oxide

4 Conclusion

The function of MRAM failed at 400 Gy(Si) with TID, and synergistic effects tests under two different radiation sources. The reason of the functional failure was STI leakage, leading to the deterioration of CMOS peripheral control circuitry. I_{SB}, I_{DDR}, and I_{DDW} varied in the test, so these parameters were regarded as the radiation-sensitive parameters that validated that the radiation damage of synergistic effects is less than that of TID, as the additional magnetic field causes electrons to drift in the oxide, and recombine with holes, resulting in lesser oxide trapped charges of synergistic effect than with TID. A hardening technique to tolerate TID is required to be integrated onto the silicon-on-insulator (SOI) CMOS supporting circuitry in the future.

References

1. J. Stöhr, H.C. Siegmann, *Magnetism: From Fundamentals to Nanoscale Dynamics*, (Springer, New York, 2007), pp. 12–15
2. D.N. Nguyen, F. Irom, Radiation effects on MRAM. Paper presented at radiation and its effects on components and systems, Deauville, 10–14 Sept 2007. https://doi.org/10.1109/radecs.2007.5205554
3. J. Heidecker, MRAM Technology Status. (Jet Propulsion Lab, 2013), https://ntrs.nasa.gov/search.jsp?R=20140000668. Accessed 12 Feb 2014
4. J. Heidecker, G. Allen, D. Sheldon, Single event latchup (SEL) and total ionizing dose (TID) of a 1 Mbit magnetoresistive random access memory (MRAM). Paper presented at radiation effects data workshop (REDW), denver, 20–23 July 2010. https://doi.org/10.1109/redw.2010.5619499
5. R. R. Katti, J. Lintz, L. Sundstrom, et al., Heavy-ion and total ionizing dose (TID) performance of a 1 Mbit magnetoresistive random access memory (MRAM). Paper presented at radiation effects data workshop, Quebec, 20–24 July 2009. https://doi.org/10.1109/redw.2009.5336307
6. S. Gerardin, A. Paccagnella, Present and future non-volatile memories for space. Trans. Nucl. Sci. **57**, 3016–3039 (2010). https://doi.org/10.1109/tns.2010.2084101
7. J. Lu, On the radiation effect in nanostructures related to nanomagnetics and spintronics. (DTRA, 2015), http://www.dtic.mil/dtic/tr/fulltext/u2/a616553.pdf. Accessed 28 Jun 2014
8. Y. Narita, Y. Takahashi, M. Harada et al., Soft errors in 10-nm-scale magnetic tunnel junctions exposed to high-energy heavy-ion radiation. J. Appl. Phys. **56**, 0802B4 (2017). https://doi.org/10.7567/JJAP.56.0802B4
9. C. Hafer, M. V. Thun, M. Mundie et al., SEU, SET, and SEFI test results of a hardened 16Mbit MRAM device. Paper presented at radiation effects data workshop (REDW), Tucson, AZ, 16–20 July 2012. https://doi.org/10.1109/redw.2012.6353717
10. G. Tsiligiannis, L. Dilillo, A. Bosio et al., Testing a commercial MRAM under neutron and alpha radiation in dynamic mode. Trans. Nucl. Sci. **60**, 2417–2622 (2013). https://doi.org/10.1109/tns.2013.2239311
11. M. V. O'Bryan, K. A. LaBel, S. P. Buchner et al., Compendium of recent single event effects results for candidate spacecraft electronics for NASA. Paper presented at IEEE NSREC Radiation Effects Data Workshop. Tucson, AZ, 14–18 July 2008. https://doi.org/10.1109/redw.2008.10
12. K. J. Hass, Dissertation, University of Idaho, 2007
13. Y. Conraux, J.P. Nozieres, V.D. Costa et al., Effects of swift heavy ion bombardment on magnetic tunnel junction functional properties. J. Appl. Phys. **93**, 7301–7303 (2003). https://doi.org/10.1063/1.1558659
14. H.X. Wei, J. He, Z.C. Wen et al., Effects of current on nanoscale ring-shaped magnetic tunnel junctions. Phys. Rev. B. **77**, 134432 (2008). https://doi.org/10.1103/PhysRevB.77.134432
15. J.R. Schwank, M.R. Shaneyfelt, D.M. Fleetwood et al., Radiation effects in MOS oxides. Trans. Nucl. Sci. **55**, 1833–1853 (2008). https://doi.org/10.1109/tns.2008.2001040
16. X. Wu, W. Lu, S. B. Xi et al., Total ionizing dose effect on 0.18 m narrow-channel NMOS transistors. Acta Phys. Sinica **62,** 136101 (2013). (in Chinese) https://doi.org/10.7498/aps.62.136101
17. S.M. Sze, K.K. Ng, *Physics of semiconductor devices* (Wiley, New York, 2006), p. 240
18. N. Alimardani, Dissertation, Oregon State University, 2014
19. G. Vincent, A. Chantre, D. Bois, Electric field effect on the thermal emission of traps in semiconductor junctions. J. Appl. Phys. **50**, 5484–5487 (1979). https://doi.org/10.1063/1.326601
20. R.P. Feynman, R.B. Leighton, M. Sands, *The Feynman Lectures on Physics*. *Mainly electromagnetism and matter*. (Addison-Wesley, Redwood City, 1969), p. 216